


 Cite this: *RSC Adv.*, 2021, 11, 10381

Received 4th February 2021

Accepted 5th March 2021

DOI: 10.1039/d1ra00943e

[rsc.li/rsc-advances](http://rsc.li/rsc-advances)

# High NH<sub>3</sub>-SCR reaction rate with low dependence on O<sub>2</sub> partial pressure over Al-rich Cu-\*BEA zeolite†

 Yusuke Ohata,<sup>a</sup> Takeshi Ohnishi,<sup>a</sup> Takahiko Moteki<sup>ab</sup> and Masaru Ogura<sup>\*ab</sup>

Dependence of NH<sub>3</sub>-SCR reaction rate on O<sub>2</sub> partial pressure was investigated at 473 K over Cu ion-exchanged MOR, MFI, CHA and \*BEA zeolites with varying "Cu density in micropores". Among the zeolites, Cu-\*BEA zeolite demonstrated promising potential as an effective catalyst for NH<sub>3</sub>-SCR over a wide range of O<sub>2</sub> partial pressure.

Selective catalytic reduction of NO<sub>x</sub> using NH<sub>3</sub> as a reducing agent (NH<sub>3</sub>-SCR) is one of the most effective ways to remove NO<sub>x</sub> from exhausts with O<sub>2</sub>-rich compositions. A lot of catalysts for the reaction have been developed, such as V-based mixed oxides, Fe-zeolites, and Cu-zeolites.<sup>1</sup> Among the catalysts so far, Cu-zeolites exhibit a high reaction rate at a low NO<sub>2</sub> concentration (standard SCR) in a low temperature region (below 550 K).<sup>1</sup> Therefore, the current central trend of the study on the catalysts for NH<sub>3</sub>-SCR is based on Cu-zeolites. Since the development of Cu/SSZ-13 zeolite catalyst with CHA topology, which exhibits a high reaction rate in wide temperature region, high selectivity of N<sub>2</sub>, and a high durability under hydrothermal conditions,<sup>2</sup> a wide variety of zeolites were tested toward the application of NH<sub>3</sub>-SCR.<sup>3</sup>

In the catalytic activity tests of NH<sub>3</sub>-SCR, it is often the case that the O<sub>2</sub> concentration in the reaction feed is fixed at a certain value,<sup>3,4</sup> and the effect of O<sub>2</sub> partial pressure ( $P_{O_2}$ ) on the reaction rate has attracted little attention. The current application of NH<sub>3</sub>-SCR is mainly the removal of NO<sub>x</sub> emitted from diesel engine. The emission contains an excess amount of O<sub>2</sub> (typically 2–17%).<sup>5</sup> A portion of the O<sub>2</sub> contained in the exhaust is steadily consumed over other catalysts for exhaust purification processes (*e.g.*, diesel oxidation catalyst; DOC and diesel particulate filter; DPF).<sup>6</sup> The DOC catalyst plays a role in oxidative removal of unburned hydrocarbon (HC) and carbon monoxide (CO) using O<sub>2</sub>. Particulate matter (PM) is trapped on the DPF and eliminated by catalytic combustion using O<sub>2</sub> and NO<sub>x</sub>. In the exhaust purification system of diesel engine, such DOC and DPF units are generally mounted at the upstream of the SCR catalyst. The state-of-the-art SCR system of diesel

engines tends to be integrated to DPF to make the whole system compact.<sup>7</sup> Moreover, the application of exhaust gas recirculation (EGR) system, which introduces a part of exhaust into engine cylinder to make the temperature of combustion decrease, resulting in the decrease of thermal NO<sub>x</sub>, is in progress for the combustion process.<sup>8</sup> These purification technologies will make the temperature of exhaust and the concentration of O<sub>2</sub> lower than they are.

On the other hand, a recent fundamental research<sup>9</sup> has shown that the reaction rate for NH<sub>3</sub>-SCR over Cu-SSZ-13 zeolite catalyst is greatly influenced by the  $P_{O_2}$  in a low  $P_{O_2}$  region with practical conditions ( $P_{O_2} < 18$  kPa)<sup>5</sup> at 473 K, where the overall rate of this reaction is largely affected by the oxidation of Cu ion on zeolites by O<sub>2</sub>.<sup>10</sup> It is shown in the literature<sup>9</sup> that the SCR rate increases with increasing Cu volumetric density. However, the significant rate drop at the  $P_{O_2}$  below 15 kPa is a common behaviour of Cu-SSZ-13 zeolite regardless of its composition. Considering the recent trends on the composition of emission from practical diesel engines and the behaviour of Cu-SSZ-13 zeolite catalyst described above, it will be desired to widen the active window for exhaust composition at low reaction temperatures (~473 K) to pass future regulations.<sup>11</sup>

Herein, a comparative study is conducted regarding NH<sub>3</sub>-SCR reaction rate dependence on the  $P_{O_2}$  at 473 K over Cu ion-exchanged MOR, MFI, CHA and \*BEA zeolites from the viewpoint of "Cu density in micropores"<sup>12</sup> to understand the effect of zeolite topology on the dependence.

Details on the preparation of the catalysts and the measurement of the reaction rates have been written in our previous reports.<sup>12,13</sup> The reaction rate was calculated by determining the amount of NO converted to N<sub>2</sub> per second, which was divided by the amount of Cu in the catalyst. The O<sub>2</sub> concentration was kept at 5% during the pretreatment at 873 K, followed by cooling the temperature to 473 K. The cooling to 473 K was conducted under the feed of NH<sub>3</sub>-SCR reactants and at least 45 min since the temperature was set to 473 K was ensured

<sup>a</sup>Institute of Industrial Science, The University of Tokyo, Komaba, Meguro, Tokyo 153-8505, Japan. E-mail: oguram@iis.u-tokyo.ac.jp

<sup>b</sup>Elements Strategy Initiative for Catalysts and Batteries, Kyoto University, Katsura, Kyoto 615-8520, Japan

† Electronic supplementary information (ESI) available. See DOI: 10.1039/d1ra00943e



to reach stable temperature and steady-state NO conversion. Then, the O<sub>2</sub> concentration was altered from 1 to 15%, and more than 10 min was needed to reach initial steady-state NO conversion at each targeted O<sub>2</sub> concentration. Formed NO<sub>2</sub> was transformed to NO by a NO<sub>2</sub> converter catalyst unit attached to a chemical luminescence NO<sub>x</sub> analyser (HORIBA VA-3000); therefore, the NO conversion detected by the analyser was regarded as the NO<sub>x</sub> conversion and the effect of background NO<sub>2</sub> was eliminated.

First of all, the catalytic activity of a reference Cu-SSZ-13 catalyst<sup>14</sup> with a similar composition to the state-of-the-art commercial catalyst for NH<sub>3</sub>-SCR was measured. It is reported that the catalyst has the composition of Si/Al and Cu/Al ratios ~9.5 and 0.3, respectively, corresponding 3.1 wt% Cu,<sup>15</sup> whose Cu content is higher than that of any catalyst used in the report<sup>9</sup> on dependence of NH<sub>3</sub>-SCR rates on O<sub>2</sub> pressure.

Fig. 1a shows the rate dependence on P<sub>O<sub>2</sub></sub> for NH<sub>3</sub>-SCR per Cu ((mole NO to N<sub>2</sub>) per (mole Cu) per s) by a kinetic measurement at 473 K over the reference Cu-SSZ-13 catalyst. Similar to “Langmuirian dependence” shown in the previous report by Jones *et al.*,<sup>9</sup> a monotonic increase of SCR rate along with P<sub>O<sub>2</sub></sub> was observed. Note that the dependence obtained in this work could be expressed by the Langmuir–Freundlich equation better than the Langmuir equation (Fig. S1†). The reaction order with respect to O<sub>2</sub> for NH<sub>3</sub>-SCR per Cu was determined according to the following power law model equation.<sup>4a</sup>

$$(\text{NH}_3\text{-SCR rate per Cu}) = A_0 \times \exp(-E_{\text{app}}/RT) \times (P_{\text{O}_2})^\alpha$$

The  $\alpha$  in this equation expresses the reaction order for O<sub>2</sub>. Fig. 1a was re-plotted to log–log axes (Fig. 1b) to know the slope corresponding to  $\alpha$ . As shown in Fig. 1b, the log–log plot did not follow a linear relationship. It is observed that the slope of the plot decreased with increase in P<sub>O<sub>2</sub></sub> in the reaction flow. This result shows that the reaction order for O<sub>2</sub> decreases with increase in P<sub>O<sub>2</sub></sub>.

This phenomenon can be explained by the suggested redox mechanism between Cu<sup>+</sup> and Cu<sup>2+</sup> in the micropore of zeolites. The reduction of Cu<sup>2+</sup> to Cu<sup>+</sup> is thought to proceed by NH<sub>3</sub> + NO co-reductants,<sup>16</sup> and the oxidation of Cu<sup>+</sup> to Cu<sup>2+</sup> is thought to proceed by O<sub>2</sub> oxidant.<sup>17</sup> It has been observed by several *operando* analyses that both Cu<sup>+</sup> and Cu<sup>2+</sup> exist under a steady-state NH<sub>3</sub>-SCR condition,<sup>18</sup> although the ratio between two oxidation states depends both on the composition of Cu-zeolites and the

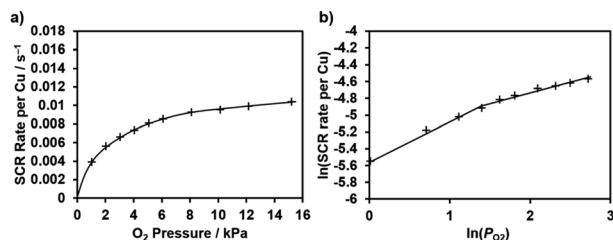


Fig. 1 (a) The dependence of NH<sub>3</sub>-SCR rate per Cu at 473 K on O<sub>2</sub> pressure and (b) the log–log plot for the calculation of apparent O<sub>2</sub> order over the reference Cu-SSZ-13 zeolite.

Table 1 The reaction order for O<sub>2</sub> at 473 K over several P<sub>O<sub>2</sub></sub> region

| O <sub>2</sub> partial pressure region/kPa | Reaction order for O <sub>2</sub> |
|--|-----------------------------------|
| 1–4  | 0.46                              |
| 5–15                                       | 0.14                              |

reaction conditions. From these results, it has been suggested that the reaction rate is not solely limited by the rate for the Cu<sup>2+</sup> reduction step (reduction half-cycle) nor Cu<sup>+</sup> oxidation step (oxidation half-cycle).<sup>10</sup> In other words, the reduction and oxidation half-cycles are kinetically relevant under the conditions below 523 K and at 5–20 kPa O<sub>2</sub> pressure over Cu-SSZ-13 zeolite.<sup>10</sup>

From the description above, the phenomenon observed in Fig. 1b can be understood as follows; the reaction is strongly influenced by the oxidation half-cycle under a low P<sub>O<sub>2</sub></sub> reaction condition because the supply of oxidant is relatively insufficiency, and the oxidation half-cycle rate is improved with increasing the P<sub>O<sub>2</sub></sub>. The reaction order for O<sub>2</sub> could be calculated in the low P<sub>O<sub>2</sub></sub> region ( $\leq 4$  kPa) and high P<sub>O<sub>2</sub></sub> region ( $5 \leq P_{\text{O}_2} \leq 15$  kPa). The results are shown in Table 1. The reaction order for O<sub>2</sub> decreased with increasing P<sub>O<sub>2</sub></sub>, but did not reach to zero-order in the P<sub>O<sub>2</sub></sub> region in this work. It is indicated from the results that the effect of oxidation half-cycle on the whole reaction rate remains in all the P<sub>O<sub>2</sub></sub> region in this work, and the effect becomes stronger in a lower P<sub>O<sub>2</sub></sub> region below 5 kPa than in the higher P<sub>O<sub>2</sub></sub> region over this Cu-SSZ-13 catalyst. The apparent activation energy ( $E_{\text{app}}$ ) for the reaction around 473 K calculated from the Arrhenius plots (Fig. S2†) was not changed obviously (Table 2) in the P<sub>O<sub>2</sub></sub> region between 1 and 15 kPa. The value of the  $E_{\text{app}}$  was typical for the NH<sub>3</sub>-SCR over Cu-zeolite catalysts.<sup>4</sup> Therefore, it is confirmed that alteration of the reaction condition does not change the apparent  $E_{\text{app}}$  for kinetically relevant step(s).

The same measurements were conducted over the Cu-zeolite catalysts with MOR, MFI, \*BEA, and CHA topologies that have similar cation density in micropores of zeolites and several Cu density in micropores.<sup>11,12</sup> Cu-Zeolites with different topologies and cation density in micropores were applied in this study to minimize the contributions from factors other than the topology that can affect the NH<sub>3</sub>-SCR rate.<sup>12</sup> Fig. 2 show the dependence of NH<sub>3</sub>-SCR rate per Cu at 473 K on P<sub>O<sub>2</sub></sub> over each topology. Cu density in micropores increases with light-to-dark shading (Table S1†). As shown in Fig. 2, monotonic increase of

Table 2 The apparent activation energy around 473 K in several O<sub>2</sub> pressure reaction over the reference Cu-SSZ-13 catalyst

| O <sub>2</sub> partial pressure/kPa | $E_{\text{app}}/\text{kJ mol}^{-1}$ |
|-------------------------------------|-------------------------------------|
| 1                                   | 49                                  |
| 5                                   | 44                                  |
| 15                                  | 44                                  |



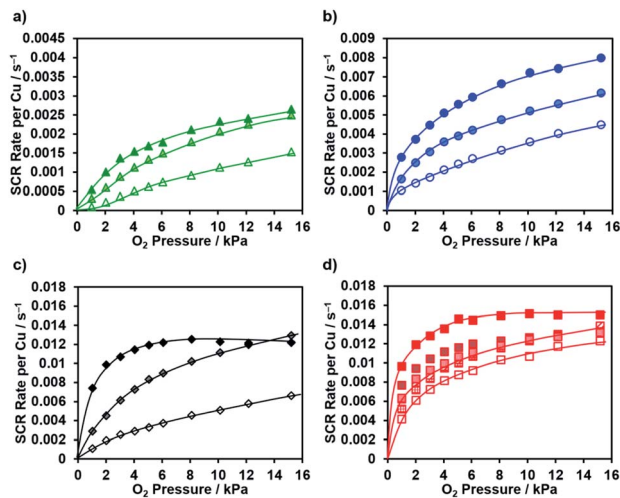


Fig. 2 The dependence of NH<sub>3</sub>-SCR rate per Cu at 473 K on O<sub>2</sub> pressure over (a) MOR, (b) MFI, (c) CHA, and (d) \*BEA zeolite catalyst with several Cu density in micropores. Cu density in micropores increases with light-to-dark shading.

SCR rate along with  $P_{O_2}$  increase similar to shown in Fig. 1a was observed over all Cu-zeolites. However, the changes of SCR rate along with both  $P_{O_2}$  and Cu density strongly affected by zeolite topologies and Cu density in micropores.

Cu-MOR zeolite applied in this study exhibited the lowest NH<sub>3</sub>-SCR rate per Cu over all  $P_{O_2}$  region (Fig. 2a). Note that the scale of Y axis in Fig. 2a is as large as a quarter of Fig. 1a. A little increase was observed in both magnitudes and slopes of NH<sub>3</sub>-SCR rate per Cu along with increasing Cu density in micropores. However, the rate was far smaller than that of the reference Cu-SSZ-13 zeolite catalyst, even with the higher Cu density.

Cu-MFI zeolite used in this study exhibited a higher NH<sub>3</sub>-SCR rate per Cu over all  $P_{O_2}$  region than Cu-MOR zeolite (Fig. 2b). The scale of Y axis in Fig. 2b is as large as a half of that in Fig. 1a. In the case of the MFI zeolite, the increase was also observed in both magnitudes and slopes of NH<sub>3</sub>-SCR rate per Cu with increasing Cu density in micropores. Both the reaction rate and its increase over Cu-MFI zeolite were larger than over Cu-MOR zeolite. However, the reaction rate over Cu-MFI zeolite was smaller than over the reference Cu-SSZ-13 zeolite catalyst regardless of Cu density in micropores. Even the Cu-MFI zeolite with Cu density in micropores at  $7.4 (1000 \text{ \AA}^3)^{-1}$  (approximately 3 times as large as the reference Cu-SSZ-13 zeolite) did not represent an exception.

In the case of Cu-CHA zeolite, the increase behaviour in NH<sub>3</sub>-SCR rate per Cu along with  $P_{O_2}$  was largely affected by the Cu density in micropores (Fig. 2c). The catalyst with a low Cu density in micropores showed relatively steady increase in NH<sub>3</sub>-SCR rate per Cu along with  $P_{O_2}$ . On the other hand, the catalyst showed the rapid increase in NH<sub>3</sub>-SCR rate per Cu in low  $P_{O_2}$  region, and the rate became constant in the higher  $P_{O_2}$  region (>6 kPa). Note that the slight decrease in NH<sub>3</sub>-SCR rate per Cu of the Cu-CHA zeolite with the largest Cu density in micropores over 8 kPa  $P_{O_2}$  region is mainly caused by the increase in the formation of N<sub>2</sub>O. Interestingly, the zeolites with Cu density in

micropores at 1.6 and  $3.4 (1000 \text{ \AA}^3)^{-1}$  exhibited almost the same NH<sub>3</sub>-SCR rate per Cu when  $P_{O_2}$  was at 15 kPa. This result suggests that they would reach the zero-order dependence on  $P_{O_2}$ , which means that the oxidation half-cycle does not determine the overall rate in the  $P_{O_2}$  region regardless of Cu density in micropores.

Among the Cu-zeolite catalysts, Cu-\*BEA zeolite employed in this study exhibited high NH<sub>3</sub>-SCR rate per Cu with relatively low dependence of on  $P_{O_2}$  (Fig. 2d). Moreover, the effect of Cu density in micropores of the catalyst was small on the behaviour of the rate along with  $P_{O_2}$ . Surprisingly, even the Cu-\*BEA zeolite catalyst with Cu density in micropores at  $0.76 (1000 \text{ \AA}^3)^{-1}$  (The sample shown as hollow red square symbol in Fig. 2d and described as B12 in Table S1†) exhibited a higher NH<sub>3</sub>-SCR rate per Cu than the reference Cu-SSZ-13 catalyst with Cu density in micropores at  $2.7 (1000 \text{ \AA}^3)^{-1}$  (Fig. S3a†). This difference was more obvious in lower temperature region (Fig. S3b†). In other words, the Cu-\*BEA zeolite catalyst exhibited a high NH<sub>3</sub>-SCR rate per Cu with low dependence on both Cu density in micropores and  $P_{O_2}$  in the temperature region below 473 K.

In the case of the zeolites other than Cu-CHA, the obvious deviation from a linear relationship following a Langmuir equation was observed in the dependence of SCR rate on  $P_{O_2}$  (Fig. S4†). To analyze the relationship, the Langmuir-Freundlich equation, which introduced the order on  $P_{O_2}$  as a correction factor to the Langmuir equation, was needed. From these results, it is suggested that the dependence of SCR rate on  $P_{O_2}$  over Cu-zeolites generally follows the Langmuir-Freundlich equation.

The reaction order for O<sub>2</sub> was calculated in a similar manner as the reference Cu-SSZ-13 catalyst in a low  $P_{O_2}$  region ( $\leq 5$  kPa). The results were displayed as a function of Cu density in micropores (Fig. 3a). As shown in Fig. 3a, the reaction order for O<sub>2</sub> decreased with increase in the Cu density in micropores for all the zeolites investigated in this study. This result was consistent with the previous report on Cu-SSZ-13 zeolites with several Cu densities<sup>18</sup> and can be understood by the increase in the rate for the oxidation half-cycle with increasing Cu density in micropores. When the reaction order for O<sub>2</sub> was compared among the Cu-zeolites with a similar Cu density in micropores, the tendency was observed that Cu-zeolite with a high reaction

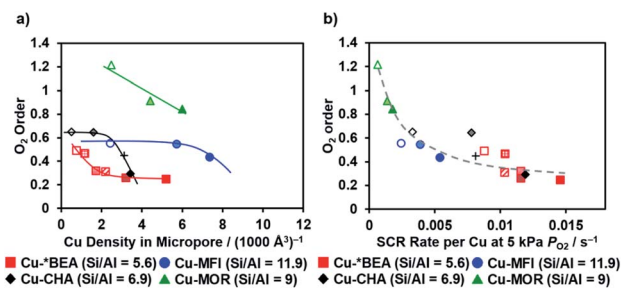


Fig. 3 The relationship between reaction order for O<sub>2</sub> in the O<sub>2</sub> pressure region ( $\leq 5$  kPa) and the (a) Cu density in micropores or (b) SCR rate per Cu at 5 kPa O<sub>2</sub> over the MOR ( $\blacktriangle$ ), MFI ( $\bullet$ ), \*BEA ( $\blacksquare$ ), and CHA ( $\blacklozenge$ ) zeolites. The cross symbol (+) shows the reference Cu-SSZ-13 zeolite.



rate showed a low reaction order for O<sub>2</sub> (Fig. 3b). This result means that the effect of P<sub>O<sub>2</sub></sub> on the reaction rate is small over a catalyst with a high reaction rate such as Cu-CHA with high Cu density in micropores or Cu-\*BEA.

Both the Cu density in micropores and P<sub>O<sub>2</sub></sub> could play a role in the oxidation half-cycle in recently suggested mechanism of NH<sub>3</sub>-SCR.<sup>17</sup> Moreover, we have reported that the dependence of SCR rate against Cu density in micropores are related to the oxidation half-cycle in a previous report,<sup>12</sup> which investigated SCR rate at O<sub>2</sub> partial pressure of 5 kPa over the same catalysts tested in this study in detail. Thus, it can be assumed that the high NH<sub>3</sub>-SCR rate of Cu-\*BEA catalyst shown in this report is derived from the oxidation property for Cu<sup>+</sup> ion by O<sub>2</sub> even insensitive to the P<sub>O<sub>2</sub></sub>. However, detailed analysis using *operando* spectroscopic techniques will be necessary to elucidate the origin. It will be reported and discussed in the closest future.

Dependence of NH<sub>3</sub>-SCR rate on P<sub>O<sub>2</sub></sub> was investigated at 473 K over Cu ion-exchanged MOR, MFI, CHA and \*BEA zeolites with several "Cu density in micropores". The reaction rate with respect to P<sub>O<sub>2</sub></sub> was largely affected by the zeolite topology. Among the zeolites investigated here, Cu-\*BEA zeolite catalyst exhibited a higher reaction rate regardless of the Cu density in micropores (or Cu loading) than a Cu-SSZ-13 reference catalyst in the whole range of Cu content tested in this study. The Cu-\*BEA zeolite has a promising potential as the effective catalyst for NH<sub>3</sub>-SCR in a wide range of P<sub>O<sub>2</sub></sub>.

## Conflicts of interest

There are no conflicts to declare.

## Acknowledgements

This work was supported by "Elements Strategy Initiative for Catalysts & Batteries (ESICB)" of MEXT; Ministry of Education, Culture, Sports, Science and Technology, Japan, Grant Number JPMXP0112101003.

## Notes and references

- 1 C. Görsmann, *Johnson Matthey Technol. Rev.*, 2015, **59**, 139.
- 2 J. H. Kwak, R. G. Tonkyn, D. H. Kim, J. Szanyi and C. H. F. Peden, *J. Catal.*, 2010, **275**, 187.
- 3 (a) M. Moliner, C. Franch, E. Palomares, M. Grillb and A. Corma, *Chem. Commun.*, 2012, **48**, 8264; (b) D. Jo, T. Ryu, G. T. Park, P. S. Kim, C. H. Kim, I.-S. Nam and S. B. Hong, *ACS Catal.*, 2016, **6**, 2443; (c) S. V. Priya, T. Ohnishi, Y. Shimada, Y. Kubota, T. Masuda, Y. Nakasaka, M. Matsukata, K. Itabashi, T. Okubo, T. Sano, N. Tsunoji, T. Yokoi and M. Ogura, *Bull. Chem. Soc. Jpn.*, 2018, **91**, 355; (d) J. Zhu, Z. Liu, L. Xu, T. Ohnishi, Y. Yanaba, M. Ogura, T. Wakihara and T. Okubo, *J. Catal.*, 2020, **391**, 346.
- 4 (a) F. Gao, E. D. Walter, E. M. Karp, J. Luo, R. G. Tonkyn, J. H. Kwak, J. Szanyi and C. H. F. Peden, *J. Catal.*, 2013, **300**, 20; (b) S. A. Bates, A. A. Verma, C. Paolucci, A. A. Parekh, T. Anggara, A. Yezerets, W. F. Schneider, J. T. Miller, W. N. Delgass and F. H. Ribeiro, *J. Catal.*, 2014, **312**, 87.
- 5 İ. A. Reşitoğ, K. Altinişik and A. Keskin, *Clean Technol. Environ. Policy*, 2015, **17**, 15.
- 6 B. K. Yun and M. Y. Kim, *Appl. Therm. Eng.*, 2013, **50**, 152.
- 7 G. Cavataio, J. R. Warner, J. W. Girard, J. Ura, D. Dobson and C. K. Lambert, *SAE Int. J. Fuels Lubr.*, 2009, **2**, 342.
- 8 M. Zheng, G. T. Reader and J. G. Hawley, *Energy Convers. Manage.*, 2004, **45**, 883.
- 9 C. B. Jones, I. Khurana, S. H. Krishna, A. J. Shih, W. N. Delgass, J. T. Miller, F. H. Ribeiro, W. F. Schneider and R. Gounder, *J. Catal.*, 2020, **389**, 140.
- 10 C. Paolucci, J. R. Di Iorio, W. F. Schneider and R. Gounder, *Acc. Chem. Res.*, 2020, **53**, 1881.
- 11 C. H. F. Peden, *J. Catal.*, 2019, **373**, 384.
- 12 Y. Ohata, H. Kubota, T. Toyao, K. Shimizu, T. Ohnishi, T. Moteki and M. Ogura, *Catal. Sci. Technol.*, 2021, DOI: 10.1039/D0CY01838D.
- 13 Y. Ohata, T. Nishitoba, T. Yokoi, T. Moteki and M. Ogura, *Bull. Chem. Soc. Jpn.*, 2019, **92**, 1935.
- 14 Detail on the preparation of the reference Cu-SSZ-13 is shown in the ESI for ref. 12. This sample is denoted as C905 in ref. 12.
- 15 J. Luo, F. Gao, K. Kamasamudram, N. Currier, C. H. F. Peden and A. Yezerets, *J. Catal.*, 2017, **348**, 291.
- 16 C. Paolucci, A. A. Parekh, I. Khurana, J. R. Di Iorio, H. Li, J. D. Albarracin Caballero, A. J. Shih, T. Anggara, W. N. Delgass, J. T. Miller, F. H. Ribeiro, R. Gounder and W. F. Schneider, *J. Am. Chem. Soc.*, 2016, **138**, 6028.
- 17 C. Paolucci, I. Khurana, A. A. Parekh, S. Li, A. J. Shih, H. Li, J. R. Di Iorio, J. D. Albarracin-Caballero, A. Yezerets, J. T. Miller, W. N. Delgass, F. H. Ribeiro, W. F. Schneider and R. Gounder, *Science*, 2017, **357**, 898.
- 18 C. Liu, H. Kubota, T. Amada, K. Kon, T. Toyao, Z. Maeno, K. Ueda, J. Ohyama, A. Satsuma, T. Tanigawa, N. Tsunoji, T. Sano and K. Shimizu, *ChemCatChem*, 2020, **12**, 3050.

